CALM WATER PERFORMANCE OF HARD-CHINE VESSELS IN SEMI-PLANING AND PLANING REGIMES

Parviz Ghadimi [1]
Sasan Tavakoli [1]
Abbas Dashtimanesh [2]
[1] Amirkabir University of Technology, Islamic Republic of Iran
[2] Persian Gulf University, Islamic Republic of Iran

ABSTRACT

In the current paper, a mathematical model is developed for performance prediction of hard-chin boats which can be used in both semi-planing and planing regimes. The proposed model bases on the 2D+T theory and implements pressure distributions over the length of the hull in order to compute the forces. To determine the forces in the semi-planing range, a function is proposed for the non-dimensional length at which the transom effect appears. Three drag components, which are: frictional drag, induced drag, and spray drag, are considered in the computations performed using an iterative method to satisfy two equilibrium equations. The validity of the proposed method is verified by comparing the predicted trim angle and resistance against the available experimental data. Based on this comparison, it is observed that the proposed method reveals satisfying accuracy in both semi-planing and planing regimes. The method is then used to study variation of hydrodynamic and hydrostatic forces as the hull makes a transition from the semi-planing regime to the planing regime. In addition, different components of the resistance are analyzed.

Keywords: hard-chine vessels, planing and semi-planing regimes, performance prediction, 2D+T theory

NOMENCLATURE

B	Boat beam
c	Half-wetted beam of 2D section (m)
c	Time rate of half-wetted beam of 2D section (m/s)
c*	Lateral position reached by whisker spray (m)
CF	Frictional resistance coefficient
CΔ	Load Coefficient
Dp	Drag acting on pressure area (N)
Ds	Drag acting on spray area (N)
L	Lift force (N)
LC	Chine wetted length (m)
LK	Keel wetted length (m)
LM	Mean wetted length (m)
LCB	Longitudinal center of hydrostatic force (m)
LCHD	Longitudinal center of hydrodynamic force (m)
LCG	Longitudinal center of gravity (%L from transom)
FB2D	2D hydrostatic force (N/m)
FB	Hydrostatic force (N)
fHD2D	2D hydrodynamic force (N/m)
FHD	Hydrodynamic force (N)
FnB	Beam Froude Number
Gξζ	Body fixed coordinate

MB	Hydrostatic moment (N-m)
MHD	Hydrodynamic moment (N-m)
OXZ	Moving coordinate
p	Pressure (Pa)
R	Reduction function
Re	Reynolds Number
Sp	Pressure area (m2)
SS	Spray area (m2)
t	Time (s)
tCW	Chine wetting time (s)
tf	Final time of solution (s)
U	Vessel speed (m/s)
w	Water impact speed (m/s)
x	Distance of section from water intersection (m)
y	Lateral distance from wedge apex
α'	Non-dimensional position at which reductions appear
β	Deadrise angle (°)
Δ	Weight (N)
ρ	Water density (Kg/m3)
	Water impact flow potential
τ	Trim angle (deg)

INTRODUCTION

Nowadays, hard-chine hulls are broadly used for recreational, sport, and military purposes. The presence of a chine in the transverse section of the hull results in flow separation from the chine and generation of the hydrodynamic force. This hydrodynamic force supports the boat weight and leads to the reduction of the wetted surface of the boat, thus dramatically diminishing the wave making resistance. All these together help the boat reach a high-speed. An important problem regarding the hydrodynamics of a hard-chine vessel is computation of its resistance and trim angle in steady motion. It can be solved through establishing the dynamic equilibrium. Overall, all earlier models focusing on the performance prediction in calm water have highlighted the planing regime. In the current paper, a model is introduced which predicts performance of the boat in both, the semi-planing and planing regimes.

The first model to predict the performance of a planing boat was presented by Savitsky (1964) who introduced some empirical relations for hydrodynamic and hydrostatic lift forces, as well as for the center of pressure of the hard-chine planing boat. This model was further developed three times by Savitsky. Firstly, Savitsky and Brown (1974) modified it to consider the effects of trim tabs and non-monohedral hull form. Later, Savitsky et al. (2007) presented new relations for considering the whisker spray drag in the initial model (1964). Finally, Savitsky (2012) widely studied a warped hull form by modifying his early model. Overall, the Savitsky method was not introduced to analyze the pre-planing regime and its use is only limited to the planing regime. Since the Savitsky method is empirical and the equations are valid for Froude numbers suitable in the planing regime, this method cannot be used for modeling both planing and semi-planing regimes. In order to analyze these two regimes simultaneously, some other options should be taken into account. It is noteworthy however, that some empirical methods for modeling hard-chine boats in semi-planing regimes are already known. Mercier and Savitsky (1973) presented empirical relations for determining the resistance of semi-planing hulls, in which they used curve-fitting. Some other research activities related to the prediction of dynamic equilibrium of planing hulls have been conducted with the emphasis on warped hull planing hulls ((Bertorello and Olivero (2007); Schachter et al. (2016)). In recent years, Radojcic et al. (2014a and 2014b) developed relations for the resistance of such a hull by applying artificial neural networks.

Computational fluid dynamics (CFD) schemes can be considered a good approach for determining the dynamic equilibrium of the planing hull and may provide adequate accuracy (Brizolla and Sera (2007)). Different researchers have achieved good accuracy in predicting the trim angle of the planing hull by using CFD (Brizzolara and Villa (2010); Garu et al. (2012); Mousavirad et al. (2015); Jiang et al. (2016)). However, it should be pointed out that while the accuracy of CFD solutions is good and reasonable, they are time consuming and cannot be easily used in the early stage design. Therefore, mathematical methods are considered a good alternative and viable option.

On the other hand, the 2D+T theory and the water entry problem together have received huge attention from the researchers. Applying this theory can help solve different hydrodynamic problems, ranging from steady motion (Vorous (1996); Savander (1997); Zhao et al. (1997); Xu and Troesch (1997); Katayama et al. (2006); Brogolia and Iafrati (2010); Ghadimi et al. (2016a)) to unsteady motions in waves (Martin (1976a,b); Zarnick (1978,1979); Akers (1999); Garme and Rosen (2003); Sebastiani et al. (2008); Faltinsen and Sun (2011); Kanayoo et al. (2015) ; Haase (2015a); Ghadimi et a. (2016b, c)).Beyond this, in some of the recent research works, forces and moments acting on a planing hull exhibiting roll (Tavakoli et al. (2015); Ghadimi et al. (2016d)) and yawed motions (Tascon et al. (2009); Morabito et al. (2015)) have also been analyzed. The potential of the 2D+T theory for modeling different motions and conditions has been realized because of recent advances in studying the water entry problem. The initial point in this regards refers to the early research of von Karman (1929) who proposed using momentum variation of a wedge entering the water for finding the normal force acting on it. Later, such research workers as Wagner (1932) made attempts to modify the von Karman (1929) study. In the last two decades, different researchers have presented innovative approaches for compaction of forces in different conditions, with the emphasis on their applications for hydrodynamic modeling of planing hulls. For example, Korobkin (2013) mentioned that his work had been motivated by the 2D+T theory. Another example is the research by Tassin et al. (2014) who mentioned that their method had been developed in such a way that the hydrodynamic force acting on a planing hull is determined using the 2D+T theory. The works by Xu et al. (1999), Judge et al. (2004), Riccardi and Iafrati (2004), and Fairlie-Clarke and Tvietnes (2008) are other examples in this regard. In the recent years, Sun and Faltinsen (2012) determined the forces acting on a boat in a semi-planing range. On the other hand, Kim et al. (2013) predicted the performance of the round bilge boat in a semi-planing regime using the2D+T theory.

In the current paper, the 2D+T theory is used to compute the performance of a hard chine boat in both semi-planing and planing regimes. The hydrodynamic forces are computed using the pressure distribution over the body. The boundary condition is implemented in each section in order to find the half wetted beam. The pressure is integrated and subsequently the hydrostatic pressure is taken into account. The performance of the boat is determined using two equilibrium equations. To consider the semi-planing regime in the computations, it is proposed to use a specific function for the longitudinal position, in which the transom effect appears. The validity of the proposed method is assessed by comparing the computed trim angle and resistance against the published experimental data. Also, a worked example is included as Appendix A, which explains in more detail particular solution steps to the analyzed problem.

THEORETICAL APPROACH

PROBLEM DEFINITION

It is assumed that a hard chine boat is moving forward with a speed U in steady condition and it has no oscillatory motion, as shown in Fig. 1. By assuming that the boat speed is categorized in both semi-planing and planing regimes, the boat is free to have a dynamic trim angle (τ) and rise up (Z_{CG}). In this situation, the boat has the keel wetted length (L_K) and the chine wetted length (L_C), which can be observed in the top view of the boat.
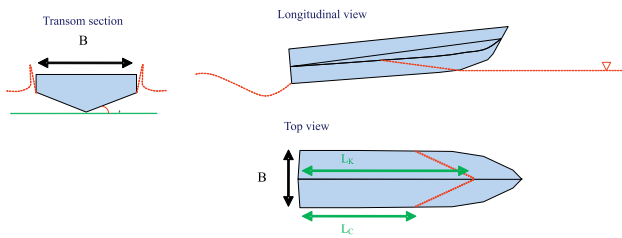
Fig. 1. Steady motion of a hard-chine boat in semi-planing and planing regimes.

MOTION EQUATION

To establish the motion equation, two coordinate systems are considered. One of them is the body-fixed coordinate system ($G\xi\zeta$) located at the center of gravity (CG). The ξ-axis is parallel to the base line and positive forward. The ζ-axis is normal to the base line and positive downward. The second system (OXZ) is a right-handed coordinate system moving with the forward speed of the boat and has no motion. The origin of this coordinate system is located at the intersection of the calm water surface by the normal line to the water passing through CG. The X-axis is parallel to the calm water surface and positive forward, while the Z-axis is normal to the calm water surface and positive downward.
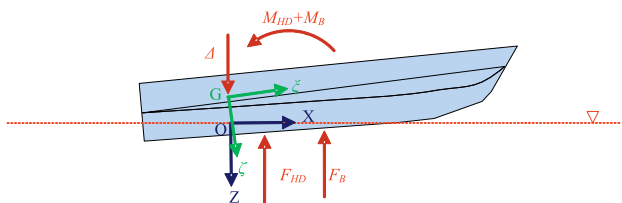
Fig. 2. Illustration of the coordinate systems and forces acting on the hard chin boat.

Forces and moments acting on the boat are shown in Fig. 2. They include the hydrodynamic force (F_{HD}), the buoyancy force (F_B), and their moments (M_{HD} and M_B). After considering that the drag and thrust forces have no contribution in the motion equation, the motion equation in steady condition can be written as

$$\sum F_Z = 0 \quad \rightarrow W - F_{HD} - F_B = 0$$
$$\sum M_G = 0 \quad \rightarrow M_{HD} + M_B = 0, \tag{1}$$

where the first equation refers to the equilibrium in Z direction and the second equation indicates the equilibrium of the pitch moments about CG. To find the equilibrium condition, it is necessary to determine these forces. In the current paper they are determined using the 2D+T theory.

2D+T THEORY

It is assumed that the boat has no oscillatory motion and passes through a transverse plane, as illustrated in Fig. 3. The problem can be changed to a water entry problem with speed of w which can be found by
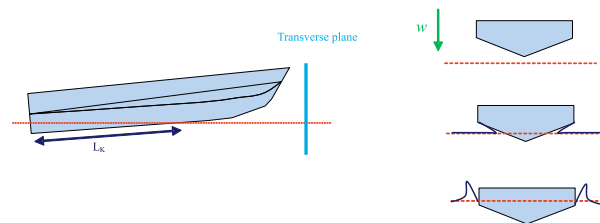
$$w = U \tan \tau, \tag{2}$$

Fig. 3. Illustration of application of the 2D+T theory for solving the steady problem related to a hard chine boat in semi-planing and planing regimes.

The flow around the wedge sections can be solved through different approaches, making use of numerical methods (Zhao et al (1993); Maki et al. (2011); Ghadimi et al. (2012); Piro and Maki (2013); Ghadimi et al. (2013); Ghadimi et al. (2014a); Abraham et al. (2014); Farsi and Ghadimi (2014a and b); Facci et al. (2015 and 2016); Farsi and Ghdimi (2015); Shademani and Ghadimi (2016); Nguyen and Park (2016); Feizi Chekab et al. (2016)), and analytical methods (Mei et al. (1999); Yottu et al. (2007); Ghadimi et al. (2011); Tassin et al. (2014)). In the current paper, the analytical methods are utilized. By assuming that the fluid is perfect, the solution of the water entry problem can be written in the form:

$$\phi = w\sqrt{c^2 - y^2}, \tag{3}$$

where c is the transverse position of the spray root and y is the lateral distance from the apex, as displayed in Fig. 4.
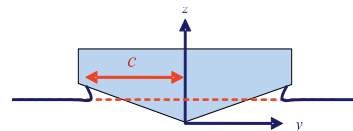

Fig. 4. Schematic of the wedge section entering the water.

Using the Bernoulli equation, the pressure acting on the section may be found as

$$p = \rho\left[\frac{wc\dot{c}}{\sqrt{c^2 - y^2}} - \frac{w^2}{2}\frac{y^2}{c^2 - y^2}\right]. \tag{4}$$

To determine the pressure, the values of c and are required. It is considered that the wedge experiences two phases, with dry chine or wet chine, as presented in Fig. 5. During the dry chine phase, these two parameters are found by

$$c = \frac{\pi}{2} \frac{wt}{\tan \beta}, \tag{5}$$

$$\dot{c} = \frac{\pi}{2} \frac{w}{\tan \beta}, \tag{6}$$

As the chines become wet, these two parameters are computed from the equations proposed by Algarin and Tascon (2014) as:

$$c = \sqrt{\left(\frac{b}{2}\right)^2 + \left[\frac{3}{2}\left[w\left(\frac{B}{2}\right)^2(t - t_{CW})\right]\right]}, \tag{7}$$

$$\dot{c} = \frac{w^2}{2} \frac{\left(\frac{B}{2}\right)^2}{c\sqrt{c^2 - \left(\frac{B}{2}\right)^2}}, \tag{8}$$

where t_{CW} is the time spray root reaching the knuckles and can be found by

$$t_{CW} = \frac{\frac{B}{2}\tan \beta}{w}. \tag{9}$$

Dry chine phase   Wet chine phase
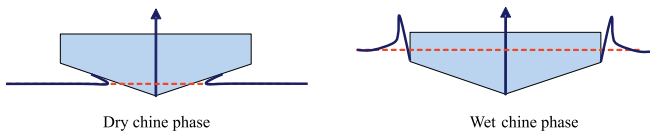
Fig 5. Illustration of phases in solving the steady problem.

It should be mentioned that Equations (7) and (8) are established by implementing the boundary condition at chines, as proposed by different researchers, for instance Korobkin and Malenica (2005).

The vertical hydrodynamic force () acting on each section may be found by integrating the pressure over the wedge wall as follows:

$$f_{HD}^{2D} = \int p \cos \beta dy, \tag{10}$$

The 2D hydrostatic force () acts on the section which may be computed using the wetted area of each section. This force can be considered in the fully planing regime through the 2D+T theory (Sun and Faltinsen (2011); Akers (2014); Kanyoo et al. (2015); Haase et al. (2015)) and through empirical equations (Korovin Kroukovski et al. (1949); Savitsky et al.

(1964); Morabito (2010, 2014); Ghadimi et al. (2015b)), and also in the semi planing regime (Sun and Faltinsen (2012); Kim et al. (2013)). Before the chine is wetted, this force may be determined by

$$f_B^{2D} = \rho g c^2 \tan \beta, \tag{11}$$

while after chine wetting, it can be estimated by

$$f_B^{2D} = \rho g \left(\frac{B}{2}\right)^2 \tan \beta. \tag{12}$$

THREE DIMENSIONAL FORCES

The three dimensional forces are computed by expanding 2D forces over the whole length of the vessel. The force due to hydrodynamic pressure is determined by

$$F_{HD} = \int_{L_K} R(\xi) f_{HD}^{2D} \cos \tau d\xi, \tag{13}$$

where $R(\xi)$ is the transom reduction function, explained in Section 2.5. The pitch moment due to hydrodynamic pressure is obtained by

$$M_{HD} = F_{HD}.LC_{HD}, \tag{14}$$

where LC_{HD} is the longitudinal position of the center of hydrodynamic force, determined by

$$LC_{HD} = \frac{\int_{L_K} R(\xi) f_{HD}^{2D} \xi d\xi}{\int_{L_K} R(\xi) f_{HD}^{2D} d\xi}. \tag{15}$$

The buoyancy force is determined by

$$F_B = \int_{L_K} R(\xi) f_B^{2D} d\xi, \tag{16}$$

and its pitching moment can be computed by

$$M_B = F_B.LC_B, \tag{17}$$

where LC_B denotes the center of buoyancy force and can be determined by

$$LC_B = \frac{\int_{L_K} R(\xi) f_B^{2D} \xi d\xi}{\int_{L_K} R(\xi) f_B^{2D} d\xi}. \tag{18}$$

TRANSOM REDUCTION

Equations (13) through (18) compose the transom reduction function. With the aid of this reduction function the forces can be predicted more accurately. The aim of using this function is to reduce the forces near the transom. In previous publications on the subject, Garme (2005) proposed a transom reduction function which can be used for 2D sections, while Morabito (2014) derived a new equation for the transom reduction function which may be used in longitudinal sections. Morabito (2015) has also emphasized the need for considering the transom reduction function when applying the 2D+T theory. It should be mentioned that in some classical works, a 3D dimensional correction factor has been used for correcting the integration of 2D force in such a way as to include transom effects. Examples of this type of correction can be found in the works of Mayo (1945), Milwitzky (1948), Schnitzer (1952), and Martin (1976a,b). Since the current research makes use of the 2D+T theory, it is preferred to use the transom reduction function proposed by Garme (2005), which can be written as

$$R(\xi) = \tanh\left[\frac{2.5}{\alpha' B \mathrm{Fn}_B}(L_K - \xi)\right], \tag{19}$$

where α' is the non-dimensional longitudinal position (from the transom) in which the reductions appears. Garme (2005) proposed that α' be set to 0.34 for the planing range. Alternatively, Kim et al. (2013) proposed α' to be equal to 0.6 in their research which deals with the semi-planing range. In the current paper, two new functions are proposed for . After assuming that the hydrodynamic forces appear at $\mathrm{Fn}_B=1$, two linear functions are proposed for α'. The first function is proposed for the hydrostatic force and has the form:

$$\alpha' = \begin{cases} 0.34(\mathrm{Fn}_B - 1) & 1 < \mathrm{Fn}_B < 2 \\ 0.34 & \mathrm{Fn}_B > 2, \end{cases} \tag{20}$$

while the second function, proposed for the hydrodynamic force, is

$$\alpha' = \begin{cases} 1 - 0.66(\mathrm{Fn}_B - 1) & 1 < \mathrm{Fn}_B < 2 \\ 0.34 & \mathrm{Fn}_B > 2, \end{cases} \tag{21}$$

Variation of α' as a function of the beam Froude number is displayed in Fig. 6.
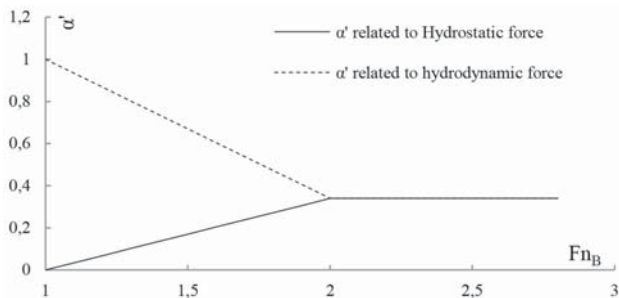
Fig 6. α' as function of FnB.

RESISTANCE

The resistance of the boat is assumed to be a combination of frictional and hydrodynamic forces. The frictional resistance acts on both the pressure area, and the spray area. The frictional coefficient is computed from the ITTC 57 formula as

$$C_F = \frac{0.075}{(\log_{10}\mathrm{Re} - 2)^2}. \tag{22}$$

Subsequently, the drag forces acting on the pressure area and the spray area can be computed, respectively, as

$$D_P = \frac{1}{2}\rho C_F U^2 S_P, \tag{23}$$

and

$$D_S = \frac{1}{2}\rho C_F U^2 S_S. \tag{24}$$

Here, S_P is the pressure area and may be computed by integrating the wetted length of each section as

$$S_P = \int c^* d\xi, \tag{25}$$

where

$$\begin{cases} c^* = c & t < t_{CW} \\ c^* = \dfrac{B}{2} & t > t_{CW}. \end{cases} \tag{26}$$

The drag force may also act on the spray area (Savitsky and Morabito (2011); Ghadimi et al. (2014b)). The spray area is computed using the method proposed by Savitsky et al. (2007). The resistance acting on the boat is determined by

$$R = \frac{D_P}{\cos\tau} + \frac{D_S}{\cos\tau} + F_{HD}\sin\tau \tag{27}$$

where the final term refers to the induced drag (drag due to the hydrodynamic force).

CHINE WETTED LENGTH

The chine wetted length of the boat is determined using the relation

$$L_C = (t_F - t_{CW})U, \tag{28}$$

where t_F is the final time for solving the water entry problem, computed based on the keel wetted length. The mean wetted length of the boat is determined by

$$L_M = \frac{L_K + L_C}{2}. \tag{29}$$

COMPUTATION PROCESS

In order to solve the steady motion of a hard-chine boat in both semi-planing and planning regimes, two systems of Equations (1) need to be satisfied. This is done using an iterative method. First, the trim angle (τ) and the keel wetted length (L_K) are guessed and then the impact velocity is computed using Equation (2). Subsequently, the time duration is determined as

$$t_F = \frac{L_K \cos \tau}{U}. \tag{30}$$

The problem is solved from 0 to t_F and the hydrodynamic pressure is computed. Because of the utilization of the 2D+T theory, each solution time is converted to a longitudinal position by applying

$$\xi = -\left(L_K - \frac{vt}{\cos \tau} \right) + LCG. \tag{31}$$

At this stage, it is checked whether or not the heave equation is satisfied. If not, the keel wetted length should be modified and re-guessed. Subsequently, it is also checked whether or not the pitch equation is satisfied. If not, the trim angle should also be re-guessed. A schematic of the computational process is shown in Fig. 7. Also, to facilitate understating of the proposed method, a worked example of application of the proposed method and its successive steps are demonstrated in Appendix A.

VALIDATION

The proposed method was validated by comparing the computed trim angle and resistance against the available experimental results. Accordingly, three steps were considered for assessing the accuracy of the method. To begin with, the planing hull series tested by Fridsma (1969) were considered, for which the trim angle and the resistance were computed. The obtained values of these parameters were compared against the experimental results in order to assess how accurately the proposed method can model these parameters for the prismatic planing hull series. In the second step, the USA coast Guard planing hull series was used as another reference for validating the obtained results. The experimental work dealing with the performance of a prismatic planing hull series was conducted by Metcalf et al. (2005). It can be considered a modern experimental effort. In addition, this planing hull series has different principal characteristics from those of the Fridsma series (1969). Finally, a planing hull with varied deadrise angle in its longitudinal direction was modeled. Positive validation of the proposed model through this step has made the precision in predicting calm water performance of a realistic (non-prismatic) hull form with the aid of the proposed model more convincing.

FRIDSMA SERIES OF PLANING HULLS

The Fridsma series has always been considered an important benchmark for validation purposes and several researchers, Akers (1999) for instance, have validated their results against the data reported by Fridsma (1969). Accordingly, the proposed method was also firstly validated on the results measured by Fridsma (1969). In the current paper, eight cases of the Fridsma series are considered. The cases were selected in such a way that they represent different load coefficients (C_Δ), L/B, deadrise angles, and LCG, intended for computation purposes. The principal characteristics of these cases are collated in Table 1.
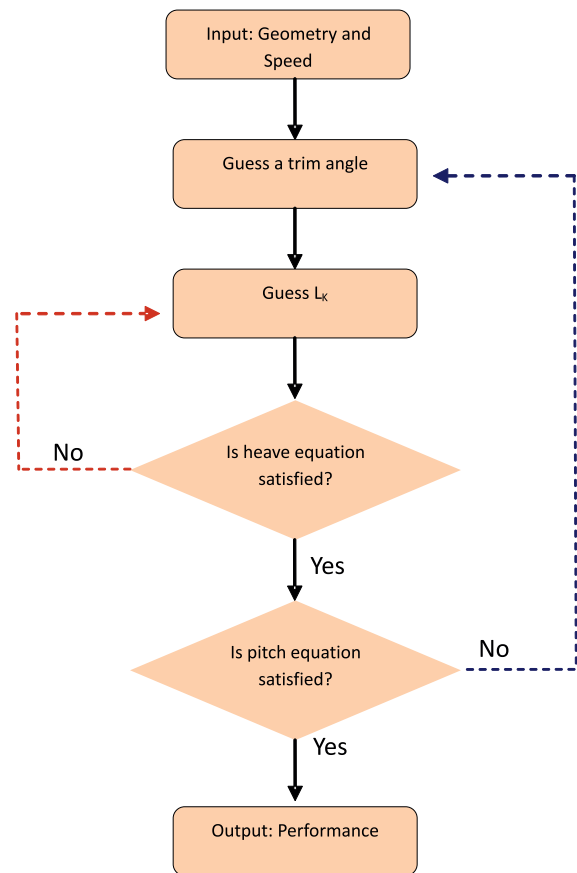
Fig. 7. *The proposed algorithm for determining the performance of a hard-chine boat in semi-planing and planing regimes.*

*Table 1. Principal characteristics of Fridsma series planing hulls.*

Case	1	2	3	4	5	6	7	8
$C_\Delta = \Delta/\rho g B^3$	0.304	0.608	0.608	0.304	0.912	0.608	0.304	0.912
Length / (m)	1.143	1.143	0.914	1.43	1.143	1.371	1.143	1.143
Beam / (m)	0.228	0.228	0.228	0.228	0.228	0.228	0.228	0.228
LCG / (%L from transom)	30	35	40	30	40	35	25	30
β	10	10	20	20	20	20	30	30

The predicted trim angles for the eight considered cases are displayed in Fig. 8. For each case, a plot of τ vs. Fn_B is presented. The targeted computations were performed for $Fn_B > 1$, to help to assess the validity of the proposed method for determining the desired parameters for both semi-planing and planing regimes. Based on the plots related to Case 1, the proposed method has revealed good accuracy in predicting the trim. Relatively speaking, the predicted trend for the trim angle is similar to that observed in the experimental results. Good accuracy observed in this case shows that the proposed method can reliably predict the performance of a hard-chine vessel with the deadrise angle of 10 degrees and light load ($C_\Delta = 0.304$) at $Fn_B > 1$. The trim angle predicted in Case 2 indicates that the precision of the current method is lower, as compared to Case 1 (This comparison is justified, as in both cases the deadrise angles are similar). The predicted trim angle at $1 < Fn_B < 2.85$ is not as good as that in Case 1. Larger weight in Case 2 ($C_\Delta = 0608$) denotes that the weight increase of a hard-chine vessel may decrease the accuracy at $Fn_B < 2.85$. It is noteworthy that the reliability of the method increases dramatically when the beam Froude number exceeds 2.85. The plots in Cases 3 through 6 correspond to the hulls with the deadrise angle of 20 degrees. Each plot shows the accuracy of the method in one particular aspect. To begin with, Case 3 represents the hard-chine hull of L/B=4 and load coefficient 0.608. According to the plots related to this case, a relatively good accuracy in predicting the trim angle is observed. Also, the behavior of the predicted trim angle as a function of the Froude number is relatively similar to the trend observed in the experimental data. Good accuracy of trim angle estimation in Case 3 indicates that the proposed method may precisely determine the trim angle of a 20 degree hard-chine hull with small L/B (L/B=4) and moderate load ($C_\Delta = 0.608$) at $Fn_B > 1$. Case 4 refers to the hard-chine boat with L/B=5 and light load ($C_\Delta = 0.608$). Comparing the predicted results related to this case against the data measured by Fridsma (1969), it can be concluded that the proposed method reveals relatively good accuracy in predicting the trim at $Fn_B > 2$. At $Fn_B = 1.33$, the accuracy is worsened, but it cannot be characterized as poor. The measured trim angle at this beam Froude number is 3.85, while the predicted

value is 3.21, which basically means that the absolute error is approximately equal to 15.9%. This error may be considered a reasonable accuracy for the semi-planing range. Case 5 refers to a 20-degree hard-chine hull with moderate L/B (L/B=5) and heavy load ($C_\Delta = 0.912$). The results of this case show good accuracy in predicting the trim angle by the proposed method. It may be noted that the predicted trim angle for the deadrise angle of 20 degrees reveals relatively good accuracy at $Fn_B > 1$ for both light-load ($C_\Delta = 0.308$, Case 4) and heavy-load conditions ($C_\Delta = 0.912$, Case 5), which is in some contrast with the results of the earlier discussed case of hard-chine hull with the deadrise angle of 10 degrees. Case 6 represents the 20-degree deadrise angle hull with large L/B (L/B=6) and light load ($C_\Delta = 0.304$). Based on the plot presented for this case, it can be concluded that the accuracy in predicting the trim angle in this case is reasonably good. The trim angle for this case is underpredicted, but the error is not large for all investigated values of Fn_B. The maximum error for the trim angle in Case 6 occurs at $Fn_B = 1.32$ and equals 10.8%. Ultimately, the accuracy of the proposed method in predicting the trim angle in Cases 7 and 8 is investigated. Both cases refer to the 30-degree hard-chine boat. In Case 7, the load is light ($C_\Delta = 0.304$) and the LCG position is 25% of boat length from the transom. Case 8 deals with heavier load ($C_\Delta = 0.304$) and the LCG position is 30% of boat length from the transom. For Case 7, the resulting plot is relatively similar to that showing the experimental results. Based on the plot in this case, the accuracy of the method in predicting the trim angle for this case is acceptable. As observed, the predicted results for all considered beam Froude numbers have approximately similar values to those recorded experimentally. This good accuracy is obvious at $Fn_B > 1$ which shows that the proposed method can be effective in reducing hydrodynamic and hydrostatic forces near the transom in the semi-planing range. With regard to the computed trim angle in Case 8, reasonably good accuracy is observed. For this case, six different runs were performed with Fn_B ranging from 1 to 2. The obtained results testify to good accuracy of the proposed method in the semi-planing regime. The error for $Fn_B = 1$ is slightly large, of about 24.3%, but it significantly decreases and approaches 7.04 percent at $Fn_B = 1.43$. There is also good accuracy for the case of $Fn_B > 2$.
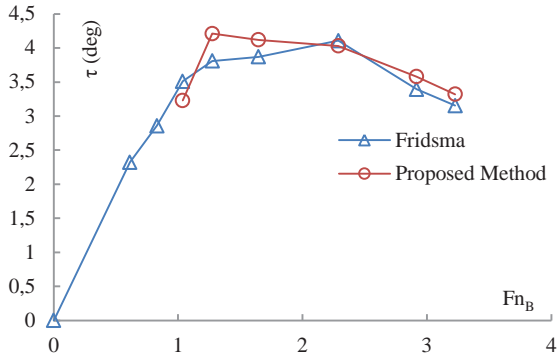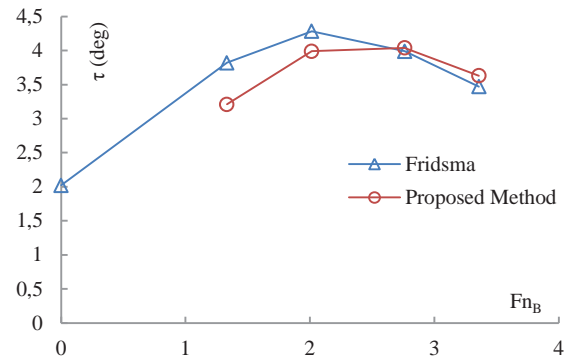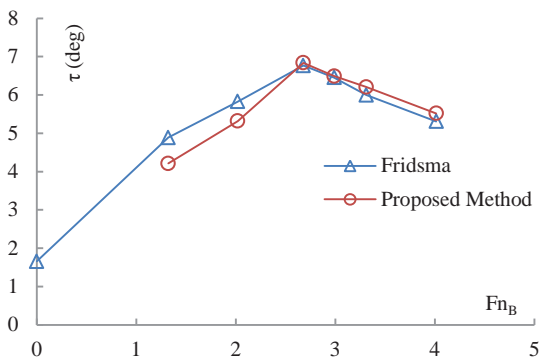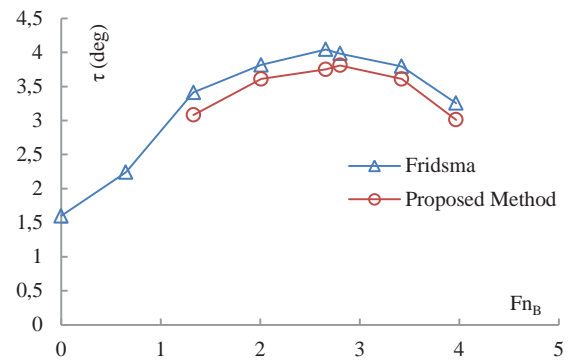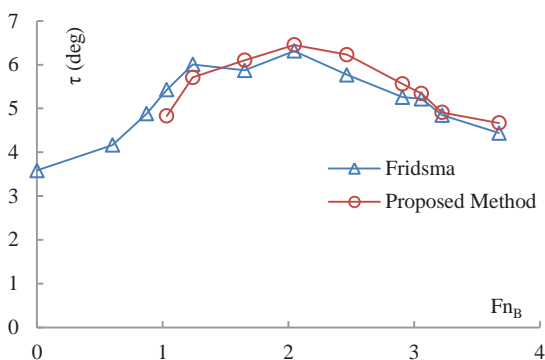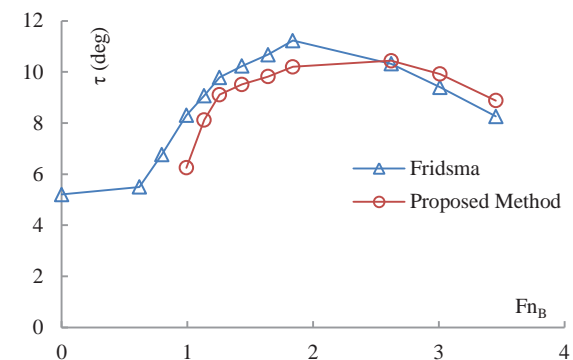
(a) Case 1
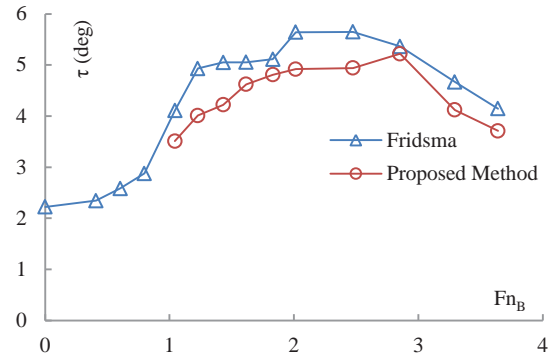
(b) Case 2
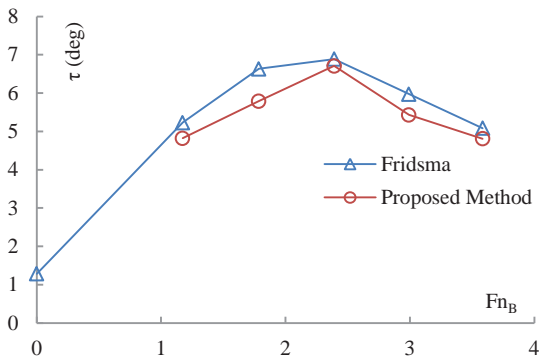
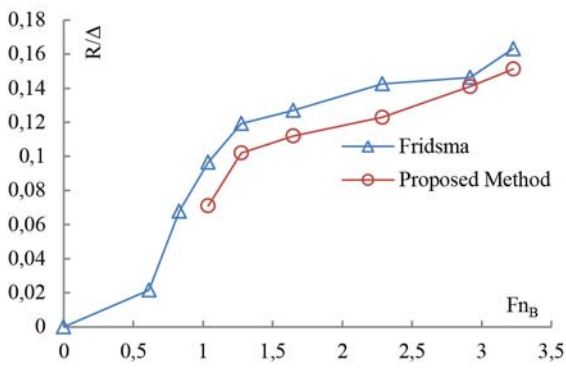(c) Case 3

(d) Case 4

(e) Case 5

(f) Case 6

(g)Case 7

(i)Case 8

Fig. 8. Comparing the predicted trim angle with the results of experimental tests of Fridsma series planing hulls
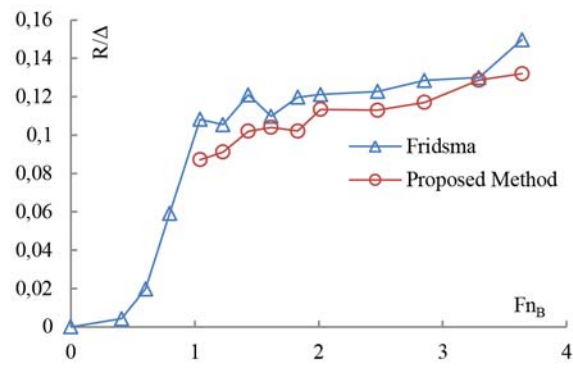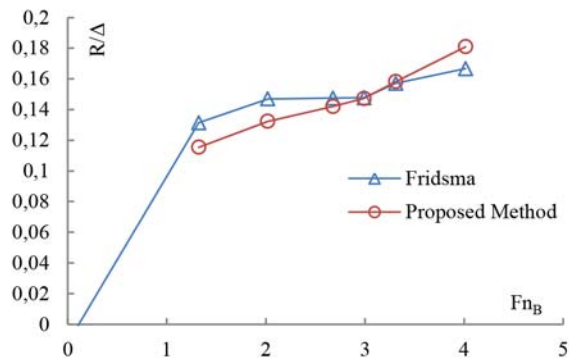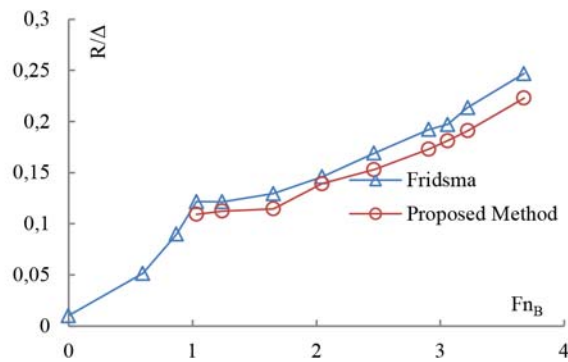
The predicted resistance of Fridsma series planing hulls is shown in Fig. 9. Everywhere in the paper, the resistance is weight normalized and computed for all 8 cases shown in Table 1. First, the resistance in Case 1 was investigated. The plot produced for this case shows that the predicted resistance is not as accurate as the trim angle (see the corresponding plot in Fig. 8). At the lowest speed, identified by FnB=1.03, the error is equal to about 26.2%. As the speed increases, the error decreases to become lower than 7.32% for FnB=3.22. The resistance in Case 2 is predicted more accurately than in Case 1. The maximum error is observed at FnB=1.04. The errors related to these two cases (Case 1 and 2) show that the current method reveals relatively good accuracy in predicting the resistance of hard-chine boats with the deadrise angle of 10 degrees. In addition, the resistance in Case 3 shows that the proposed method computes the resistance with high accuracy for FnB>1. It is noteworthy that in this case, good accuracy in predicting the trim angle is also observed (see Fig. 8). Regarding the resistance in Case 4, a similar trend is observed to that in the experimental results. It can be pointed out that the non-dimensionalized resistance is slightly underpredicted in this case. However, the errors associated with this underprediction are not so significant and the mean value of the error for this case is 11.5%, which may be considered a reasonable error in predicting

the resistance of hulls of this type in the pre-planing and planing regimes. The resistance predicted in Case 5 is not so accurate. According to the R/Δ plot displayed for this case, the predicted resistance trend differs from that observed in the experimental results. For this case, the method exhibits some uncertainties. This fact can be due to heavy weight of the boat (CΔ=0.912) and possible iteration errors which may occur when determining the hydrodynamic force contribution and the wetted length. These errors can dramatically affect the predicted wetted surface, spray area, and subsequently the resistance. It should be noted that the trim angle in this case was predicted with good accuracy, as explained earlier. Furthermore, the resistance computed in Case 6 is in good agreement with the data reported by Fridsma (1969). Also, the predicted trend is approximately similar to that observed in the experimental plot. The predicted resistances in Cases 7 and 8, which deal with the hull of 30-degree deadrise angle, reveal good conformity with the experimental data. As observed, the resulting trends for R/Δ vs. FnB are similar to the plots presented by Fridsma (1969). It is noteworthy that for 1<FnB<2 the resistance was predicted with relatively good accuracy, which indicates that the proposed method has good potential for predicting the hull resistance at the semi-planing range.
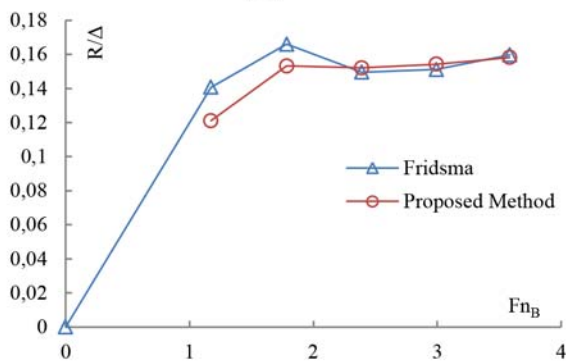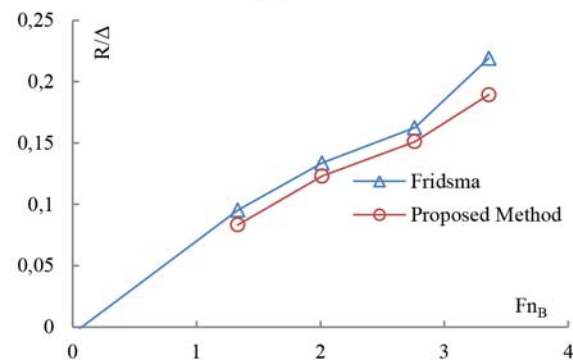
Fig. 9. Comparing the predicted resistance with the results of experimental tests of Fridsma series planing hulls.
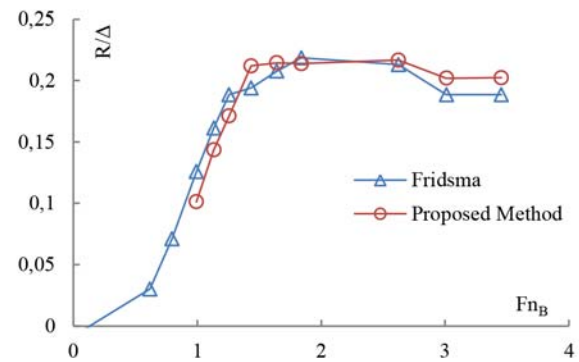
(e) Case 5
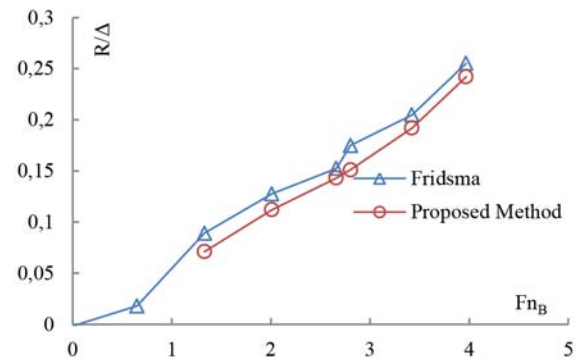
(f) Case 6

(g) Case 7

(i) Case 8

Fig. 9. Comparing the predicted resistance with the results of experimental tests of Fridsma series planing hulls.

USA COAST GUARD SERIES

After examining the accuracy of the proposed method in performance (trim angle and resistance) prediction of Fridsma series planing hulls, another prismatic hull form was examined for validation purposes. This hull series bears the name of USA Coast Guard planing hull series, and includes four different hull forms. In the current paper, two of these hulls (Model 5629 and 5631) were examined. The performances of these hulls were experimentally reported by Metcalf et al. (2005). Here, the performance of each hull was analyzed for three different load coefficients and two different longitudinal CG positions. The principal hull characteristics and the considered validation cases are shown in Table 2. These cases were selected in such a way as to allow three different load conditions to be taken into account for each hull form.

Table 2. Principal characteristics of USA Coast Guard series planing hulls.

Case	5629-1	5629-2	5629-3	5631-1	5631-2	5631-3
$C_\Delta = \Delta / \rho g B^3$	0.303	0.381	0.491	0.421	0.530	0.683
Length / (m)	3.048	3.048	3.048	3.048	3.048	3.048
Beam / (m)	0.762	0.762	0.762	0.672	0.672	0.672
LCG / (%L from transom)	38	38	38	42	42	42
β	16.61	16.61	16.61	20	20	20

Figure 10 shows the predicted trim angle for the USA Coast Guard series planing hulls. The computations, accomplished at $Fn_B > 1$, provided opportunities for assessing the accuracy of

the proposed method in both the semi-planing and planing conditions. The plots related to Model 5629 (Fig. 10a, b and c) show that the proposed method accurately determines the trim angle for this hull form at different load conditions (including 0.303, 0.381 and 0.491). The maximum error for each load is observed at the speed categorized as the semi-planing range ($1 < Fn_B < 2$). It should be noted that these errors are not significant and can be considered reasonable. In the case of load coefficient 0.303, the maximum error occurs at $Fn_B = 1.08$ and approximately equals 18.9%. The errors dramatically decrease with the speed increase. The maximum error in predicting the trim angle in the case $C_\Delta = 0.381$ is 13.4% and is observed at $Fn_B = 1.03$. In this case, the trim angle prediction error becomes smaller as Fn_B increases, which is a similar trend to that observed in the case $C_\Delta = 0.303$. Finally, the accuracy of the case with load coefficient of 0.491 is reasonably good, even at small beam Froude numbers (semi-planing regime). Overall, the observed general agreement between the trim angles predicted using the proposed method and the data reported by Metcalf et al. (2005) implies that the suggested method reveals reliable accuracy in predicting the trim angle of model 5629, which is a hard-chine hull with the deadrise angle of 16.61 degrees.

Another hull used to verify the validity of the current method is Model 5631. This hull was also studied at three different load conditions. The computed trim angle related to the first load condition of 0.421 is illustrated in Fig. 10d.

Relatively good accuracy is observed for this case, especially at $Fn_B > 2$. Although, at smaller beam Froude numbers ($Fn_B < 2$) the accuracy is not so good, the errors seem reasonable. The maximum error is observed at $Fn_B = 1.08$ and is approximately equal to 24.6%. Beyond this Fn_B, the error decreases and never becomes larger than 18.01%. The trim prediction accuracy for the load condition of 0.530 is good, as evidenced in

Fig. 10e. As observed, for all Fn_B values the predicted trim angles reveal good agreement with the experimental results. Figure 10f illustrates the computed trim angle for the case of $C_\Delta = 0.683$. The obtained plot (trim angle as a function of beam Froude number) behaves in relatively the same way as the experimental plot, which also corroborates reasonable accuracy of the proposed method.
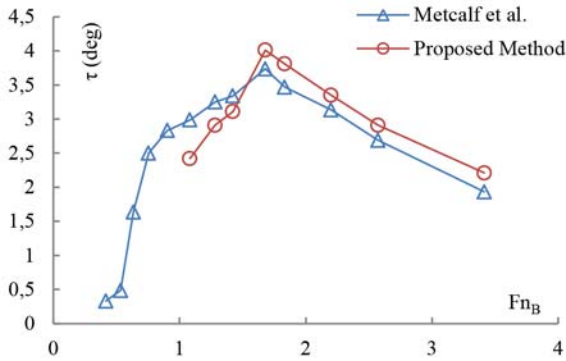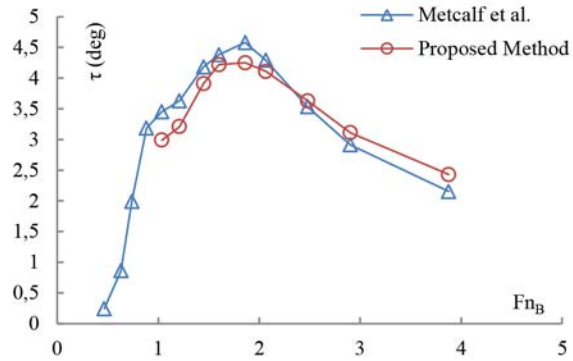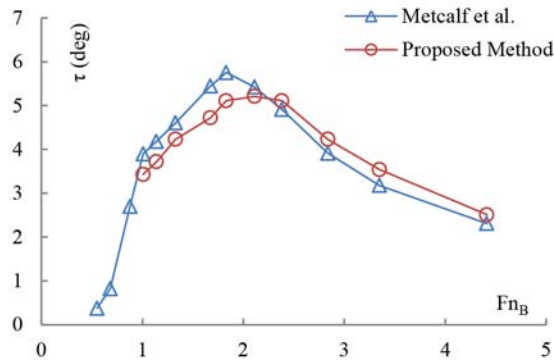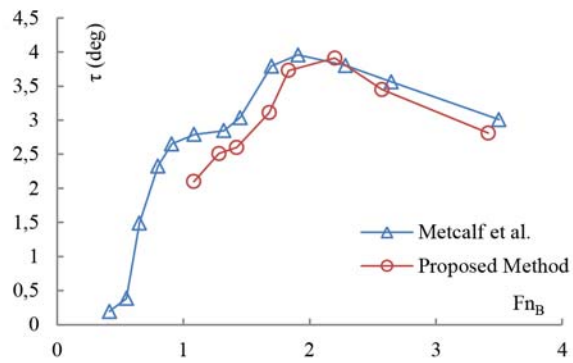
Fig. 10. Comparing the predicted trim angles with the experimental results by Metcalf et al. (2005).

The resistances computed for Models 5629 and 5631 are displayed in Fig. 11. First, the accuracy of the current method in predicting the resistance for Model 5629 is described. The plots referring to this model are presented in Fig. 11a, b and c for three different load coefficients (0.303, 0.381 and 0.491). As evident in the figure, the accuracy of the resistances calculated for load coefficients of 0.303 and 0.381 is reasonably good. The predicted R/Δ vs. Fn_B trends are similar to those observed in the experimental data, and the computed values reveal very good conformity with the results of experimental measurements by Metcalf et al. (2005). At only one speed the accuracy is slightly worse, which is the largest Fn_B for both cases. Regarding the case with load coefficient of 0.303, the observed error at Fn_B=3.41 is about 8.04%, while the error at Fn_B=3.87 for the case with load of 0.381 is 8.75%. With

regards to the predicted resistance for Model 5629 with load coefficient of 0.491, it should be noted that the accuracy in not so good. In other words, the predicted resistances for this case are uncertain since the resulting trend differs from that observed in the experimental data.

The R/Δ values calculated for Model 5631 are shown in Fig. 11d, e and f. It is noteworthy that for all three load conditions, the resistances were computed accurately. As observed, the predicted R/Δ trends are similar to those observed in the experimental plots, which confirms good agreement between the predicted and experimental results.

Overall, the observed good accuracy in resistance prediction for Models 5629 and 5631 indicates that the proposed method can reliably determine the resistances of prismatic hull forms at both planing and semi-planing ranges.
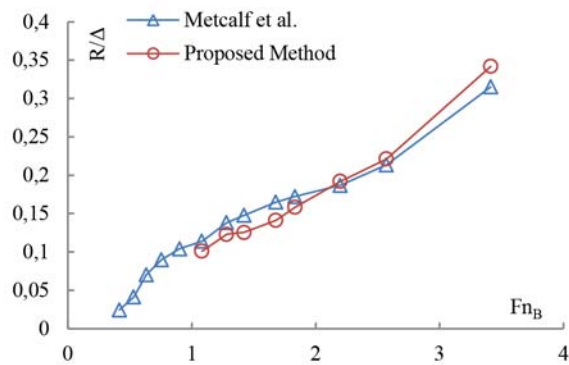
(a) Case 5629-1
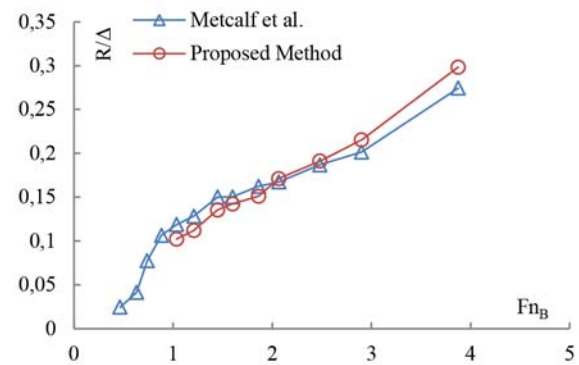
(b) Case 5629-2
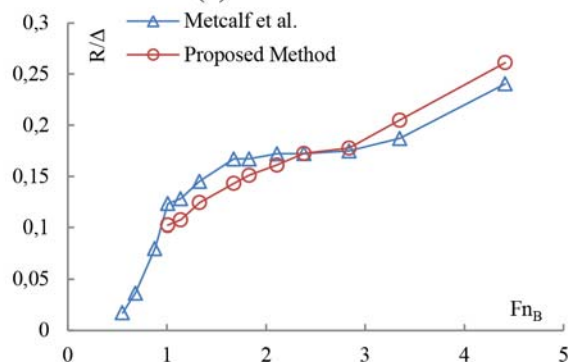
(c) Case 5629-3
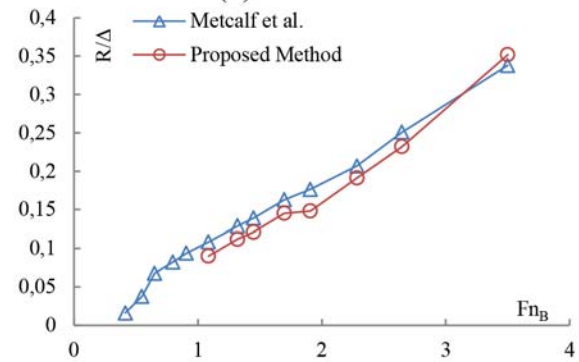
(d) Case 5631-1
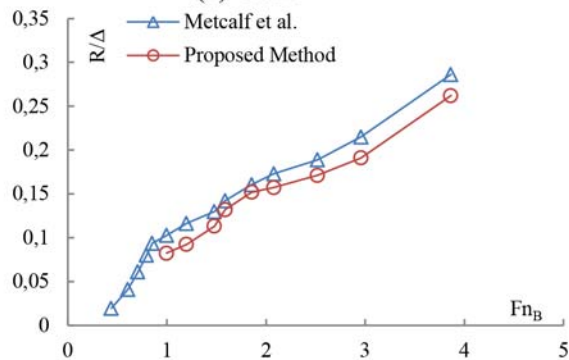
(e) Case 5631-2
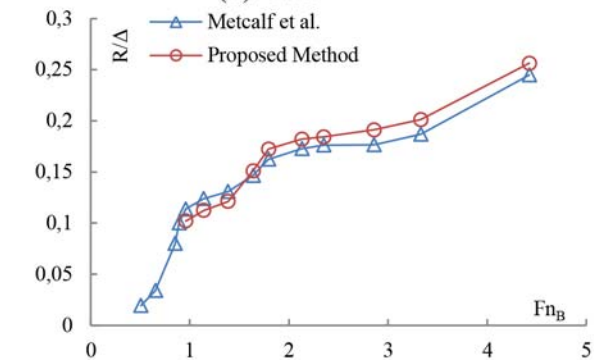
(f) Case 5631-3

Fig. 11. Comparing the predicted resistances with the experimental results by Metcalf et al. (2005).

MODEL C-SOUTHAMPTON

In addition to the two earlier examined planing hull series used for validation purposes, another planing hull series that has not a prismatic hull form was considered for further accuracy assessment of the proposed method. Validating the proposed method through the use of this hull series provides further confidence, as a more realistic hard-chine hull is mathematically modeled. That was why the planing hull series of Southampton was considered. From among all hulls existing in this series, Model C was only selected for assessing the potential of the proposed method. The trim angle reported for the other model in this series is very small (between 1 and 2 degrees) and cannot be determined using the proposed method. The principal dimension of Model C is shown in Table 3. It should be noted that this planing hull series was introduced by Taunton et al. (2010) and the performances of all hulls were measured in calm water.

Table 3. Principal characteristics of Southampton Series Model C.

Case	Model C
$C_\Delta = \Delta / \rho g B^3$	0.248
Length / (m)	2
Beam / (m)	0.46
LCG / (%L from transom)	33
β	22.5

Tauton et al. (2010) reported the performance of Model C at $Fn_B > 2$ which means that this part of validation cannot support the semi-planing range for this hull form. Figure 12 shows the predicted trim angle and R/Δ. With regard to the trim angle, it can be seen that the computed values are approximately similar to those recorded in the experiments, especially at $Fn_B > 4$. At small beam Froude numbers on this plot ($2 < Fn_B < 3$), a relatively good agreement can be observed between the predicted trim angles and the measured data. In addition, the behavior of the τ vs. FnB plot is approximately similar to the data reported by Tauton et al. (2005) at FnB>3.63. Slight differences observed between the trends of these plots at smaller Froude numbers (ranging from FnB=2.07 to 3.63) can be due to the error associated with trim angle prediction for these Froude numbers. Over this range of Froude numbers, the maximum error occurs at the smallest Froude number FnB =2.07 and is approximately equal to 16.1%. The trend observed for this range of Froude numbers can be considered the same. The resistance computed using the proposed method is in reasonable agreement with the experimental values. However, the trends are not similar. At Fn_B=3.63, a sudden resistance drop is observed, which is in contrast with the experimental plot. It is noteworthy that for this beam Froude number the trim angle also displays a sudden drop, see Fig. 12a. This trim able drop results in high decrease of the predicted keel wetted length, which dominates the computations and leads to the resistance decrease. At larger Fn_B, the resistance trends are similar. The conformity between the experimentally recorded and numerically predicted trim angle values leads to a similar resistance trend for the beam Froude number Fn_B=3.63.
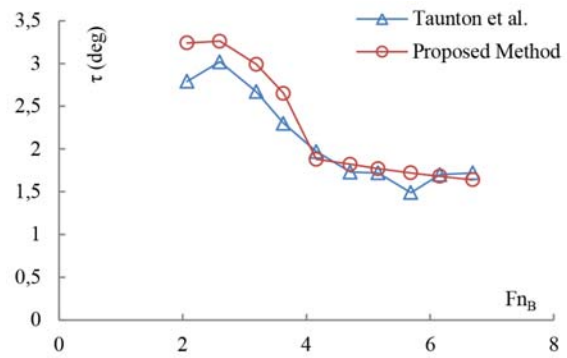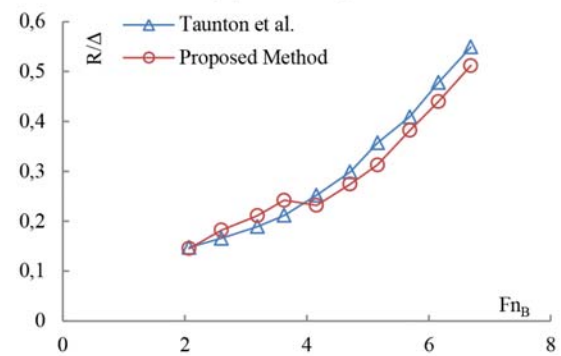
Fig. 12. Comparing the predicted trim angles and resistances with the experimental results by Taunton et al. (2010).

RESULTS OF PARAMETRIC STUDIES

The results of the conducted parametric studies are presented in two different sections. In both sections, an attempt was made to identify variations of selected parameters when the fluid at the bottom of the boat starts producing the hydrodynamic force. First, the contributions of hydrodynamic and hydrostatic forces in weight supporting were examined. Subsequently, the resistance components were studied. The studies were performed for Cases 6 and 7 of the Fridsma series, since very good accuracy was earlier observed in performance prediction of these two hulls.

CONTRIBUTION OF HYDRODYNAMIC AND HYDROSTATIC FORCES

Figure 13 shows percentage contribution of different forces at each beam Froude number. As evident in the figure, the contribution of the hydrodynamic force increases in both cases as the speed increases. The comparison between the results of these two hulls (Fig. 13a and b) implies that for Case 7, the hydrodynamic force contribution is larger at $Fn_B < 2$. This shows that for a hull with larger deadrise angle, larger hydrodynamic forces are needed to support the boat weight. A boat with larger deadrise angle has smaller hydrostatic force (because the submerged area of each section is smaller) and an additional hydrodynamic force is required.
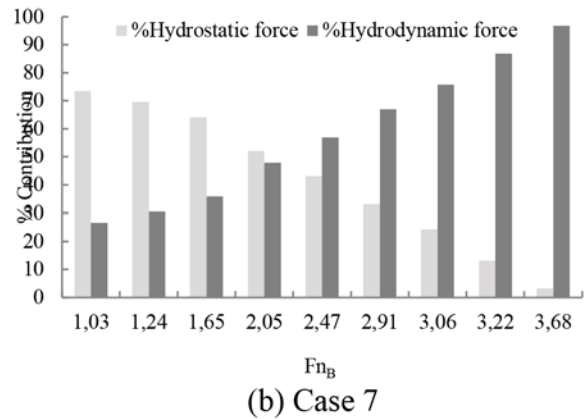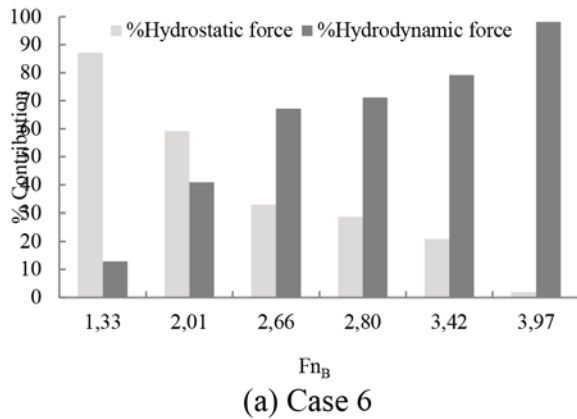
Fig. 13. Contribution of hydrodynamic and hydrostatic forces in supporting the boat weight.

RESISTANCE COMPONENTS

The resistance components for the hard-chine boats in Cases 6 and 7 are illustrated in Fig. 14. The computed data show that the spray component is initially small, but as the speed increases this component becomes larger. This trend is observed in both cases. The frictional component in Case 6 increases dramatically with the increasing Fn_B, while in Case 7 only slight increase of this component is observed. This may be due to different trim angles of the boat (see Fig.

Fig. 14. Resistance components as FnB functions.

8). The trim angle in Case 7 is larger than that in Case 6, which leads to smaller wetted surface (because the hull needs a smaller surface to produce the hydrodynamic force) and, finally, to smaller frictional resistance. The generated plots also show that the induced resistance (the resistance due to hydrodynamic force) approaches a constant value for beam Froude numbers larger than 3 and has little variation beyond this range. The observed trend implies that this component becomes fixed when the hard-chine boat reaches a specific speed and its trim angle has little variation.

5. CONCLUSIONS

The paper presents a mathematical model to determine the performance of a hard chine boat in semi-planing and planing regimes. The model is based on the 2D+T theory and makes use of pressure distributions to determine the hydrodynamic forces. Transom effects are taken into account by using well-known empirical functions. Additionally, in the semi-planing regime, a special function is proposed to compute the non-dimensional length at which the transom effect begins. The trim angle and the keel wetted length of the boat are determined by satisfying the heave and pitch equations. This task is accomplished through an iterative process. Two guesses are taken into consideration with respect to the keel wetted length and the trim angle, and the final values are determined after a number of iterations.

The validity of the method was assessed using three different hull series. For each series, the trim angle and the resistance were computed and compared with the available experimental data. Two of these series represented prismatic boats, while the third series was a boat with variable deadrise angle in longitudinal direction. Overall, good accuracy has been observed in trim angle and resistance predictions, with similar trends between the computed results and experimental data.

The proposed method was also applied to study the variation of the hydrodynamic force as a function of the beam Froude number. It was demonstrated that the hydrodynamic component is very small at lower beam Froude numbers

(slightly larger than 1.0), and then significantly increases and dominates over the supporting force generated at the bottom. Moreover, different resistance components were analyzed. It is illustrated that the spray drag component increases with the increasing speed. It is also shown that the induced drag reaches a constant value.

The future work will extend the current method towards developing a model for maneuvering of hard-chine boats, where forward acceleration of the boat and motion in horizontal plane can be targeted. For this purpose, an attempt will be made to include the semi-planing range in the planned computation.

REFERENCES

1. Abraham, J., Gorman, J., Reseghetti, F., et al., *Modeling and numerical simulation of the forces acting on a sphere during early-water entry*, Ocean Engineering, Vol. 76, 1-9, 2014.

2. Akers R.H.: *Dynamic Analysis of Planing Hulls in the Vertical Plane*, Proceedings of the Society of Naval Architects and Marine Engineers, New England Section, 1999.

3. Akers R.H.: 2014. *Advances in time-domain simulation of planing boats*. In: Proceedings of the Fourth Chesapeake Powerboat Symposium, Annapolis, MD, USA, 2014.

4. Algarin R., Tascon, O.: *Hydrodynamic Modeling of Planing Boats with Asymmetric and Steady Condition*, Proceedings of the 9th Conference on High Speed Marine Vehicles, Naples, Italy, 2011.

5. Algarin R., Tascon, O.: *Analysis of Dynamic Stability of Planing Craft on the Vertical Plane*, Ship Science and Technology, Vol. 8, No. 15, 2014.

6. Bertorello C, Olivero L.: *Hydrodynamic Resistance Assessment of non-monohedral planing hull forms based on Savitsky's methodology*, Australian Journal of Mechanical Engineering, Vol. 4, No. 2, 209-204, 2007.

7. Brizzolara S, Sera F. *Accuracy of CFD codes in the Prediction of planing surfaces hydrodynamic characteristics.* In: Proceedings of the 2nd International Conference on marine Research and Transportation, 2007.

8. Brizzolara S, Villa D., CFD simulation of planing hulls. In: Proceedings of the 7th International conference on High-Performance Marine Vehicles, Melbourne, Florida, USA, 2010.

9. Brogila R., Iafrati A.: *Hydrodynamic of planing hulls in asymmetric conditions*. In: 28th Symposium on Naval Hydrodynamics Pasadena, California, 2010.

10. Facci, A.L., Panciroli, R., Ubertini, S., Porfiri, M.,: *Assessment of PIV-based analysis of water entry problems through synthetic numerical datasets*, Journal of Fluids and Structures, Vol. 55, 484-500, 2015a.

11. Facci, A.L., Porfiri, M., Ubertini, S.: *Three-dimensional water entry of a solid body: A computational study*, Journal of Fluids and Structures, Vol. 66, 36-53, 2016.

12. Fairelie-Clarke, AC., Tvetnies T.: *Momentum and Gravity Effects During the Constant Velocity Water Entry of Wedge-Shaped Sections,* Ocean Engineering, Vol. 35, 2008.

13. Farsi, M., Ghadimi, P.: *Finding the best combination of numerical schemes for 2-D SPH simulation of wedge water entry for a wide range of deadrise angles*, International Journal of Naval Architecture and Ocean Engineering, Vol. 6, No. 3, 638-651, 2014a.

14. Farsi, M., Ghadimi, P., *Effect of flat deck on catamaran water entry through smoothed particle hydrodynamics*, Proceedings of the Institution of Mechanical Engineers Part M: Journal of Engineering for the Maritime Environment, Vol. 230, No. 2, 267-280, 2014b.

15. Farsi, M., Ghadimi, P.: *Simulation of 2D symmetry and asymmetry wedge water entry by smoothed particle hydrodynamics method,* Journal of the Brazilian Society of Mechanical Sciences and Engineering, Vol. 37, No. 3, 821-835, 2015.

16. Feizi Chekab, M.A., Ghadimi, P., Farsi, M.: *Investigation of three-dimensionality effects of aspect ratio on water impact of 3D objects using smoothed particle hydrodynamics method*, Journal of the Brazilian Society of Mechanical Sciences and Engineering, Vol. 38, No. 7, 1987-1997, 2016.

17. Fridsma G.: *A Systematic Study of the Rough-Water Performance of Planing Boats (PART I), Davidson Laboratory,* Report No. 1275, 1969.

18. Garme K.: *Improved Time Domain Simulation of Planing Hulls in Waves by Correction of Near-Transom Lift,* International Journal of Shipbuilding Progress, Vol. 52, No. 3, 2005.

19. Garme K., Rosen A.: *Time domain simulations and full-scale trials on planing crafts in waves*, International Shipbuilding progress, Vol. 50, No. 3, 177-208, 2003.

20. Garo R., Datla R., Imas L.: *Numerical simulation of planing hull hydrodynamics*. In: Proceedings of the Third Chesapeake Powerboat Symposium, Annapolis, MD, USA, 2012.

21. Ghadimi, P., Saadatkhah, A., Dashtimanesh, A.: *Analytical solution of wedge water entry by using Schwartz-Christoffel conformal mapping*, International Journal of Modeling, Simulation, and Scientific Computing, Vol. 2, No. 3,

337-354, 2011.

22. Ghadimi P., Dashtimanesh A., Djeddi S.R.: *Study of water entry of circular cylinder by using analytical and numerical solutions*, Journal of Brazilian Society of Mechanical Sciences and Engineering, Vol. 34, No. 3, 225-232, 2012.

23. Ghadimi, P., Feizi Chekab, M.A., Dashtimanesh, A.: *A numerical investigation of the water impact of an arbitrary bow section*, ISH Journal of Hydraulic Engineering, Vol. 19, No. 3, 186-195, 2013.

24. Ghadimi, P., Feizi Chekab, M.A., Dashtimanesh, A.: *Numerical simulation of water entry of different arbitrary bow sections*, Journal of Naval Architecture and Marine Engineering, Vol. 11, No. 2, 117-129, 2014a.

25. Ghadimi P., Tavakoli S, Dashtimanesh A., Pirooz A.: Developing a computer program for detailed study of planing hull's spray based on Morabito's approach. *Journal of Marine Science and Application*. Vol. 13, No. 4, 402-415. 2014b.

26. Ghadimi P., Tavakoli S., Feizi Chakab M. A., Dashtimanesh A.: *Introducing a particular mathematical model for predicting the resistance and performance of prismatic planing hulls in calm water by means of total pressure distribution*, Journal of Naval Architecture and Marine Engineering, Vol. 12, No. 2, 73-94, 2015.

27. Ghadimi P., Tavakoli S., Dashtimanesh A. Zamanian R.: *Steady performance prediction of a heeled planing boat in calm water using asymmetric 2D+T model*, Proceedings of the Institution of Mechanical Engineers, Part M: Journal of Engineering for the Maritime Environment, Published Online: 2016a. DOI: 10.1177/1475090216638680.

28. Ghadimi P, Tavakoli S, Dashtimanesh A.: *Coupled heave and pitch motions of planing hulls at non-zero heel angle.* Applied Ocean Research, Vol. 59, 286-303, 2016b.

29. Ghadimi P., Tavakoli S., Dashtimanesh A.: *An analytical procedure for time domain simulation of roll motion of the warped planing hulls.* Proceedings of the Institution of Mechanical Engineers, Part M: Journal of Engineering for the Maritime Environment, 230(4), 600-615, 2016c.

30. Ghadimi P, Tavakoli S, Dashtimanesh A. A non-linear mathematical model for coupled heave, pitch and roll motions of a high-speed planing hull, Journal of Engineering Mathematics. Published Online, 2016d. 10.1007/s10665-016-9878-2.10.1007/s10665-016-9878-2.

31. Haase H., Soproni J.P., Abdel-Maksoud M.: Numerical analysis of a planing boat in head waves using 2D+T method. Ship Technology Research, 62(3), 131-139, 2015.

32. ITTC: *Report of Resistance Committee*, 8th International Towing Tank, Madrid, Spain, 1957.

33. Conference, Venice, 2002.

34. Jiang Y., Zou, J., Hu, A., Yang J.; Analysis of tunnel hydrodynamic characteristics for planing trimaran by model test and numerical simulations, Ocean Engineering, Vol. 13, 101-110, 2016.

35. Judge C., Troesch A., Perlin M.: *Initial water Impact of a wedge at Vertical and Oblique Angles,* Journal of Engineering Mathematics, Vol. 48, 2004.

36. Kanyoo P., Taunton D., Blake J.I.: Development and optimization of mathematical model of high speed planing hulls. In: Proceedings of the 13th International Conference on Fast Sea Transportation (FAST 2015), DC, USA, 2015.

37. Katayama T., Fujimoto M., Ikeda Y.: *A study in transverse stability loss of planing craft at super high forward speed.* In: Proceedings of the 9th International Conference on Stability of Ships and Ocean Vehicles, Rio de Janerio, Brazil, 2006.

38. Korobkin A.A.: *A linearized model of water exit.* Journal of Fluid Mechanics, 737, 368-386, 2013.

39. Korobkin A.A., Melenica S.: *Modified Logvinovic model for hydrodynamic loads on asymmetric contours entering water.* In: Proceedings of the 20th International Workshop on Water Waves and Floating Bodies, Oslo, Norway, 2005.

40. Krovin-Kroukovsky B.V., Savitsky D., William L.: *Wave contours in the wake of a 20° deadrise planing surface.* Davidson Laboratory, Report No. 337, 1949.

41. Kim D.J., Rhee K.P., You Y.J.: *Theoretical Prediction of Running Attitudes of a Semi-Displacement Round Bilge Vessel at High Speed,* Applied Ocean Research, Vol. 42, 2013.

42. Maki K.J., Lee D., Troesch AW., Vlahopoulos N.: *Hydroelastic impact of a wedge-shaped body.* Ocean Engineering, Vol. 38, 621-629.

43. Martin M.: *Theoretical determination of porpoising instability of high-speed planing boat.* David Taylor Naval Ship Research and Development Center, Report No. 76-0068, 1976a.

44. Martin M.: *Theoretical prediction of motion of high-speed planing boats in waves.* David Taylor Naval Ship Research and Development Center, Report No. 76-0069, 1976b.

45. Mei X., Liu Y., On the water impact of general two-dimensional sections, Applied Ocean Research, Vol. 21, No. 1, 21-15, 1999.

46. Mercier J.A., Savitsky D.: *Resistance of Transom Shear Craft in the Pre-planing Range*, Davison Laboratory, Report No. 1667, Hoboken, NJ, USA, 1973.

47. Metcalf B.J., Faul L., Bumiller E., Slutsky, J.: *Resistance Tests of a Systematic Series of US Coast Guard of Planing Hulls,* NSWCCd-50-TR-2005/063, 2005.

48. Milwitzky B. 1948. A generalized theoretical and experimental investigation of the motions and hydrodynamic loads experienced by V-bottom seaplanes during step-landing impact. NACA TN 1516.

49. Morabito M.G.; *On the spray and bottom pressures of planing surfaces*, PhD Thesis, Stevens Institute of Technology, Hoboken, NJ, USA.

50. Morabito, M.G.; *Empirical Equations for Planing Hull Pressure Distributions.* Journal of Ship Research, Vol. 58, No. 3, 2014.

51. Morabito M.G.: *Prediction of Planing Hull Side Forces in Yaw Using Slender Body Oblique Impact Theory,* Ocean Engineering, Vol. 101, 2015.

52. Mousaviraad, S.M., Wang, Z., Stern, F.: *URANS studies of hydrodynamic performance and slamming loads on high-speed planing hulls in calm water and waves for deep and shallow conditions,* Applied Ocean Research, Vol. 51, 222-240, 2015.

53. Nguyen, V.-T., Park, W.-G.: *A free surface flow solver for complex three-dimensional water impact problems based on the VOF method*, International Journal for Numerical Methods in Fluids, Vol. 82, No. 1, 3-34, 2016.

54. Piro D.J., Maki K.J.: *Hydroelastic analysis of bodies that enter and exit water*, Journal of Fluids and Structures, Vol. 37, 134-150, 2013.

55. Riccardi G, Iafrati A.: Water impact of an asymmetric floating wedge. Journal of Engineering Mathematics, Vol. 49, 19-39, 2003.

56. Savitsky D.: *Hydrodynamic Design of Planing Hulls*, Marine Technology, Vol. 1, No. 1, 1964.

57. Savitsky D.; *The Effect of Bottom Warp on the Performance of Planing Hulls,* Proceedings of the third SNAME Chesapeake Powerboat Symposium, Annapolis, 2011.

58. Savitsky D., Brown W.: *Procedures for Hydrodynamic Evaluation of Planing Hulls in Smooth and Rough Water,* Marine Technology, Vol. 13, No. 4, 1978.

59. Savitsky D., Morabito M.,: *Origin and characteristics of the spray patterns generated by planing hulls*, Journal of Ship Production, Vol. 27, No. 2, 63-83.

60. Savitsky D., DeLorme M. F., Datla R.; *Inclusion of Whisker Spray Drag in Performance Prediction Method for High-Speed Planing Hulls,* Marine Technology, Vol. 44, No. 1, 2007.

61. Savander BR.: Planing hull steady hydrodynamics. PhD Thesis. University of Michigan, Ann Arbor, Michigan, USA, 1997.

62. Sebastiani L., Bruzzone D., Gualeni P., et al.: *A practical method for the prediction of planing craft motions in regular and irregular waves*. In: Proceedings of the ASME 27th International Conference on Offshore Mechanics and Arctic Engineering, Estoril, Portugal, 2008.

63. Schachter RD, Riberio HJC.: *Dynamic equilibrium evaluation for planing hulls with arbitrary geometry and variable deadrise angles – The virtual prismatic hulls method,* Ocean Engineering, Vol. 115, 67-92, 2016.

64. Schnitzer E, 1952. Theory and procedure for determining loads and motions in chine-immersed hydrodynamic impacts. NACA TN 2813.

65. Shademani, R., Ghadimi, P.: *Estimation of water entry forces, spray parameters and secondary impact of fixed width wedges at extreme angles using finite element based finite volume and volume of fluid methods*, Brodogradnja, Vol. 67, No. 1, 101-124, 2016.

66. Sun H., Faltinsen O.M.: *Dynamic motions of planing vessels in head seas. Journal of Marine Science and Technology*, Vol. 16, 168-180, 2011.

67. Sun H., Faltinsen O.M.: *Hydrodynamic Forces on a Semi-Displacement Ship at High Speed,* Applied Ocean Research, Vol. 34, 2012.

68. Tascon O.D., Troesch A.W., Maki K.J.: *Numerical computation of hydrodynamic forces acing on a maneuvering planing hull via slender body theory-SBT and 2-D impact theory*. In: Proceedings of the 10th International Conference on Fast Sea Transportation (FAST 2009), Athens, Greece, 2009.

69. Tassin A., Korobkin AA., Cooker M.J.: On analytical models of vertical water entry of symmetric body with separation and cavity initiation. Applied Ocean Research, 48, 33-41, 2014.

70. Tavakoli S., Ghadimi P., Dashtimanesh A., Sahoo P.K.: *Determination of Hydrodynamic Coefficients Related to Roll Motion of High-Speed Planing Hulls,* Proceedings of the 13the International Conference on Fast Sea Transportation, DC, USA, 2015.

71. Radojcic D., Zgradic A., Kalajdzic M., Simic, A., *Resistance Prediction for Hard-Chine Hulls in the Pre-Planing Regime,* Polish Maritime Research, Vol. 21, 2014a.

72. Radojcic D., Morabito M.G., Simic A. P., Zgradic A.B.: Modeling with regression analysis and artificial neural networks the resistance and trim of series 50 experiments with V-bottom motor boats, *Journal of Ship Production and Design*, Vol. 30, No. 4, 153-174, 2014b.

73. von Karman T.: *The impact on Seaplane Floats During Landing,* NACA TN 321.

74. Vorus SW.: *A flat cylinder theory for vessel impact and steady planing*, J. Ship Research, Vol. 40, No. 2, 89-106, 1996.

75. Wagner H.: *Phenomena Associated with Impacts and Sliding on Liquid Surface*, NACA Translation of Uber Stoss- und Gleitvorgange an der Oberflache von Flussigkeiten. Zeitschr. Angew. Math. Mech, Vol. 12, No, 4, 1932.

76. Xu L., Troesch A.W.; *A study on hydrodynamic of asymmetric planing surfaces.* In: Proceedings of the 5th International Conference on Fast Sea Transportation (FAST 99), Seattle, Washington, USA, 1999.

77. Xu L., Troesch A.W., Peterson R.: *Asymmetric hydrodynamic impact and dynamic response of vessels.* Journal of Offshore Mechanics and Arctic Engineering, Vol. 121, 83-89: 1999.

78. Yettou E.M., Derochers A., Champoux, Y.: *A new analytical model for pressure estimation of symmetrical water impact of a rigid wedge at variable velocities*, Journal of Fluids and Structures, Vol. 23, 502-522, 2007.

79. Zarnickh E.E.: *A nonlinear mathematical model of motions of a planing boat in regular waves.* David Taylor Naval Ship Research and Development Center, Report No. 78/032, 1978.

80. Zarnickh E.E.: *A nonlinear mathematical model of motions of a planing boat in irregular waves.* David Taylor Naval Ship Research and Development Center, Report No. SPD-0867-01, 1979.

81. Zhao R., Faltinsen O. M.: *Water entry of two-dimensional bodies.* Journal of Fluid Mechanics, Vol. 246, 593-612, 1993.

82. Zhao R., Faltinsen O. M., Haslum H.A.: *A simplified nonlinear analysis of a high-speed planing craft in calm water.* In: Proceedings of the 4th International Conference on Fast Sea Transportation (FAST 97), Sydney, Australia, 1997.

APPENDIX A: A WORKED EXAMPLE

A particular case of US Coast Guard boat series (Case 5629-1) is hereby considered to move forward at a beam Froude Number of 2.2. The boat is first divided into n sections (here, $n = 21$). The deadrise angle and the beam of each considered section are displayed in Table A. 1.

The initial trim angle (4.1 deg for this case) and the keel wetted length (0.5L for this case) are guessed. Subsequently, the 3D problem is changed to a 2D problem. From the intersection of the keel and calm water to the transom location, m sections are considered (here, $m = 51$). The longitudinal distance of each section from the keel/calm water intersection is determined. Then, the half beam (column 2) of each section and its deadrise angles (column 3) are computed. The chine depth of each section is found using the formula $\frac{B}{2} \tan \beta$ and the time of chine wetting of each section is then computed from Equation 9 (column 5). The corresponding solution time for each section is then determined using the formula $x/\cos \tau)/U$ (column 6). Afterward, it is checked to see if the time t of each section is longer or shorter than the chine wetting time. In the latter condition the section experiences phase 1 (i.e. dry chine phase); otherwise it experiences phase 2 (i.e. wet chine phase). Later, depending on the phase, Equations (5) through (8) are utilized to find c and $\dot{c}$ (columns 8 and 9).

Table A. 1. The deadrise angle and beam of each section.

Distance of section from transom (m)	Beam of section (m)	Deadrise angle of section (deg)
0	0.76	16.61
0.1524	0.76	16.61
0.3048	0.76	16.61
0.4572	0.76	16.61
0.6096	0.76	16.61
0.762	0.76	16.61
0.9144	0.76	16.61
1.0668	0.76	16.61
1.2192	0.76	16.61
1.3716	0.76	16.61
1.524	0.76	16.61
1.6764	0.76	16.61
1.8288	0.76	16.61
1.9812	0.76	16.61
2.1336	0.76	16.61
2.286	0.76	16.61
2.4384	0.76	16.61
2.5908	0.76	16.61
2.7432	0.76	16.61
2.8956	0.76	16.61
3.048	0.76	16.61

Table. A. 2. Sectional characteristics after guessing the keel wetted length.

x (m)	$B/2$ (m)	(deg)	$\frac{B}{2} \tan \beta$	t_{CW} (s)	t (s)	Phase (1 or 2?)	c (m)	$\dot{c}$ (m/s)
0	0.38	16.61	0.113355	0	0	1	0	0
0.03048	0.38	16.61	0.113355	0.167372	0.005054	1	0.011475	2.270389
0.06096	0.38	16.61	0.113355	0.167372	0.010109	1	0.022951	2.270389
0.09144	0.38	16.61	0.113355	0.167372	0.015163	1	0.034426	2.270389
0.12192	0.38	16.61	0.113355	0.167372	0.020217	1	0.045902	2.270389
0.1524	0.38	16.61	0.113355	0.167372	0.025272	1	0.057377	2.270389
0.18288	0.38	16.61	0.113355	0.167372	0.030326	1	0.068852	2.270389
0.21336	0.38	16.61	0.113355	0.167372	0.035381	1	0.080328	2.270389
0.24384	0.38	16.61	0.113355	0.167372	0.040435	1	0.091803	2.270389
0.27432	0.38	16.61	0.113355	0.167372	0.045489	1	0.103279	2.270389
0.3048	0.38	16.61	0.113355	0.167372	0.050544	1	0.114754	2.270389
0.33528	0.38	16.61	0.113355	0.167372	0.055598	1	0.126229	2.270389
0.36576	0.38	16.61	0.113355	0.167372	0.060652	1	0.137705	2.270389
0.39624	0.38	16.61	0.113355	0.167372	0.065707	1	0.14918	2.270389

0.42672	0.38	16.61	0.113355	0.167372	0.070761	1	0.160656	2.270389
0.4572	0.38	16.61	0.113355	0.167372	0.075816	1	0.172131	2.270389
0.48768	0.38	16.61	0.113355	0.167372	0.08087	1	0.183606	2.270389
0.51816	0.38	16.61	0.113355	0.167372	0.085924	1	0.195082	2.270389
0.54864	0.38	16.61	0.113355	0.167372	0.090979	1	0.206557	2.270389
0.57912	0.38	16.61	0.113355	0.167372	0.096033	1	0.218033	2.270389
0.6096	0.38	16.61	0.113355	0.167372	0.101087	1	0.229508	2.270389
0.64008	0.38	16.61	0.113355	0.167372	0.106142	1	0.240983	2.270389
0.67056	0.38	16.61	0.113355	0.167372	0.111196	1	0.252459	2.270389
0.70104	0.38	16.61	0.113355	0.167372	0.116251	1	0.263934	2.270389
0.73152	0.38	16.61	0.113355	0.167372	0.121305	1	0.27541	2.270389
0.762	0.38	16.61	0.113355	0.167372	0.126359	1	0.286885	2.270389
0.79248	0.38	16.61	0.113355	0.167372	0.131414	1	0.29836	2.270389
0.82296	0.38	16.61	0.113355	0.167372	0.136468	1	0.309836	2.270389
0.85344	0.38	16.61	0.113355	0.167372	0.141522	1	0.321311	2.270389
0.88392	0.38	16.61	0.113355	0.167372	0.146577	1	0.332787	2.270389
0.9144	0.38	16.61	0.113355	0.167372	0.151631	1	0.344262	2.270389
0.94488	0.38	16.61	0.113355	0.167372	0.156686	1	0.355737	2.270389
0.97536	0.38	16.61	0.113355	0.167372	0.16174	1	0.367213	2.270389
1.00584	0.38	16.61	0.113355	0.167372	0.166794	1	0.378688	2.270389
1.03632	0.38	16.61	0.113355	0.167372	0.171849	2	0.382988	1.702286
1.0668	0.38	16.61	0.113355	0.167372	0.176903	2	0.386488	1.142161
1.09728	0.38	16.61	0.113355	0.167372	0.181957	2	0.389188	0.951451
1.12776	0.38	16.61	0.113355	0.167372	0.187012	2	0.391488	0.844632
1.15824	0.38	16.61	0.113355	0.167372	0.192066	2	0.393588	0.771434
1.18872	0.38	16.61	0.113355	0.167372	0.197121	2	0.395488	0.718216
1.2192	0.38	16.61	0.113355	0.167372	0.202175	2	0.397388	0.673775
1.24968	0.38	16.61	0.113355	0.167372	0.207229	2	0.399088	0.639634
1.28016	0.38	16.61	0.113355	0.167372	0.212284	2	0.400688	0.611321
1.31064	0.38	16.61	0.113355	0.167372	0.217338	2	0.402288	0.586028
1.34112	0.38	16.61	0.113355	0.167372	0.222392	2	0.403788	0.564602
1.3716	0.38	16.61	0.113355	0.167372	0.227447	2	0.405288	0.545053
1.40208	0.38	16.61	0.113355	0.167372	0.232501	2	0.406688	0.528267
1.43256	0.38	16.61	0.113355	0.167372	0.237556	2	0.408088	0.512711
1.46304	0.38	16.61	0.113355	0.167372	0.24261	2	0.409388	0.499239
1.49352	0.38	16.61	0.113355	0.167372	0.247664	2	0.410688	0.486604
1.524	0.38	16.61	0.113355	0.167372	0.252719	2	0.411988	0.474719

The pressure distributions are computed in all sections using the Bernoulli equation (Equation (4)), after which the hydrodynamic force acting on each section is found. As an example, Fig. A. 1 shows the pressure distributions in four different sections: two for phase 1 and two for phase 2.

Using Equations (10) through (12), the hydrodynamic and hydrostatic forces acting on each section are computed (columns 2 and 3 in Table A. 3.). Then, the reduction magnitude in each section is computed using Equations (19) through (21) (column (4) in Table A. 3). This reduction is implemented to the sectional forces, and their values, after correction, are re-computed (columns (5) and (6) in Table A. 3). For better clarity, Fig. A. 2 shows the distributions of sectional forces in the longitudinal direction. The curves in this figure show the distributions before and after implementation of the reduction function.

Fig. A. 1. Examples of computed pressure distributions in four different sections.

| x (m)	f_B^{2D} (N/m) Without reduction	f_{HD}^{2D} (N/m) Without reduction	R(ξ)	f_B^{2D} (N/m) With reduction	f_{HD}^{2D} (N/m) With reduction
0	0	0	1	0	0
0.03048	0.160083	29.56091	0.999996	0.160083	29.56079
0.06096	0.640333	59.12181	0.999995	0.64033	59.1215
0.09144	1.44075	88.68272	0.999993	1.44074	88.6821
0.12192	2.561334	118.2436	0.999991	2.561311	118.2425
0.1524	4.002084	147.8045	0.999988	4.002037	147.8028
0.18288	5.763001	177.3654	0.999984	5.762912	177.3627
0.21336	7.844085	206.9263	0.99998	7.843926	206.9221
0.24384	10.24534	236.4872	0.999973	10.24506	236.481
0.27432	12.96675	266.0482	0.999965	12.9663	266.0389
0.3048	16.00834	295.6091	0.999955	16.00761	295.5957
0.33528	19.37009	325.17	0.999941	19.36894	325.1507
0.36576	23.052	354.7309	0.999923	23.05022	354.7034
0.39624	27.05409	384.2918	0.999899	27.05136	384.2529
0.42672	31.37634	413.8527	0.999868	31.3722	413.798
0.4572	36.01876	443.4136	0.999828	36.01255	443.3371
0.48768	40.98134	472.9745	0.999775	40.97211	472.8679
0.51816	46.26409	502.5354	0.999706	46.25047	502.3874
0.54864	51.86701	532.0963	0.999615	51.84706	531.8916
0.57912	57.7901	561.6572	0.999497	57.76105	561.375
0.6096	64.03335	591.2181	0.999343	63.99131	590.83
0.64008	70.59677	620.779	0.999142	70.53622	620.2466
0.67056	77.48035	650.3399	0.99888	77.39354	649.6113
0.70104	84.6841	679.9008	0.998536	84.56016	678.9057
0.73152	92.20802	709.4617	0.998088	92.03173	708.1054
0.762	100.0521	739.0226	0.997503	99.80226	737.1772
0.79248	108.2164	768.5836	0.996739	107.8634	766.0769
0.82296	116.7008	798.1445	0.995741	116.2037	794.7451
0.85344	125.5054	827.7054	0.994439	124.8074	823.1026
0.88392	134.6301	857.2663	0.992741	133.6528	851.0431
0.9144	144.075	886.8272	0.990526	142.7101	878.4253
0.94488	153.8401	916.3881	0.98764	151.9386	905.0613
0.97536	163.9254	945.949	0.983881	161.2831	930.7016
1.00584	174.3308	975.5099	0.978992	170.6685	955.0167
1.03632	185.0564	712.8405	0.972641	179.9934	693.3377
1.0668	196.1021	452.3537	0.964403	189.1216	436.2514
1.09728	207.468	364.6209	0.953744	197.8714	347.755
1.12776	219.1541	315.8852	0.939991	206.0028	296.9291
1.15824	231.1604	282.7139	0.92231	213.2015	260.7498
1.18872	243.4868	258.7345	0.89969	219.0625	232.7807
1.2192	256.1334	238.8104	0.870925	223.073	207.986
1.24968	269.1001	223.5712	0.834631	224.5992	186.5993
1.28016	282.3871	211.6077	0.78928	222.8824	167.0177
1.31064	295.9941	201.1609	0.7333	217.0525	147.5113
1.34112	309.9214	192.3461	0.665231	206.1693	127.9546
1.3716	324.1688	184.3318	0.583959	189.3012	107.6422
1.40208	338.7364	177.4726	0.489011	165.6457	86.78602
1.43256	353.6242	171.1347	0.380864	134.6826	65.17898
1.46304	368.8321	165.6608	0.261185	96.33339	43.2681
1.49352	384.3602	160.539	0.132899	51.08109	21.33548
1.524	400.2084	155.733	0	0	0
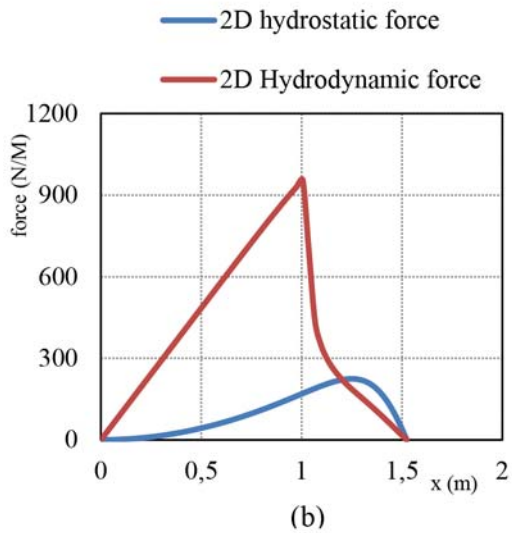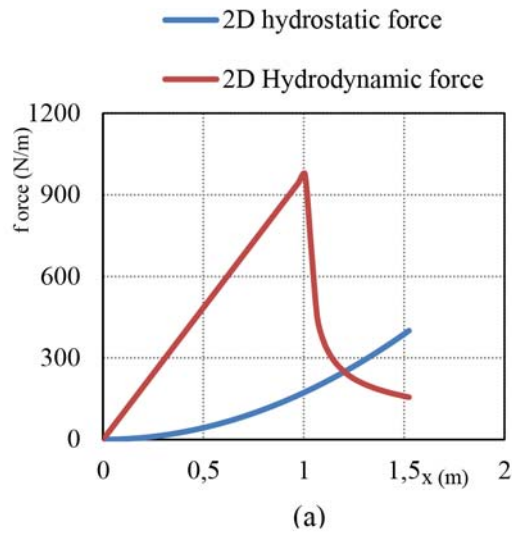
Fig. A. 2. Distribution of 2D sectional forces in longitudinal direction: without (a) and with (b) implementation of transom reduction.

The final three dimensional hydrodynamic and hydrostatic forces are subsequently found by integrating the sectional forces. Here, the trapezoidal integration method is used. It is shown that heave equation is satisfied (Δ-L=0) by checking the error for the heave force (Table A. 4.).

Table A. 4. Checking the heave force error for the guessed keel wetted length.

$F_{HD} = \int_{L_K} R(\xi) f_{HD}^{2D} \cos\tau d\xi, (N)$	606.0244
$F_B = \int_{L_K} R(\xi) f_B^{2D} d\xi, (N)$	149.8464
$L = F_B + F_{HD}(N)$	755.8708
$\varepsilon = \Delta - L(N)$	-592.1618

If the heave force error is negative the wetted length should be increased, if positive - it should be decreased. In the current example the keel wetted length is considered to increase by 0.2 m in each iteration. The results are shown in Table A. 5.

We can observe that after four iterations the error changes from negative to positive. Therefore, the correct keel wetted length is between 2.124 m and 2.324 m. Using mathematical computations, the keel wetted length for which the error approximately equals zero is found to be 2.246 m.

Table A. 5. Heave force error for different keel wetted lengths at τ=4.1.

No. of iteration	1	2	3	4	5
LK(m)	1.524	1.724	1.924	2.124	2.324
ε (m)	-592.162	-480.961	-358.071	-99.2996	63.23946

For the current wetted length, similar characteristics to those shown in Table A. 2 to A. 3 are calculated again. Then, the distance of each section from the CG is found as $\xi = -(x-L_K+LCG)$ and the sectional moments due to 2D hydrodynamic and hydrostatic forces are determined, as displayed in Table A. 6.

Table A. 6. Sectional pitch moment.

x(m)	ξ (m)	$\int_{L_K} R(\xi) f_{HD}^{2D} \xi d\xi$	$\int_{L_K} R(\xi) f_B^{2D} \xi d\xi$
0	1.2648	0	0
0.04492	1.21988	45.43183	0.362588
0.08984	1.17496	86.94973	1.387879
0.13476	1.13004	124.5537	2.982162
0.17968	1.08512	158.2438	5.051727
0.2246	1.0402	188.0199	7.502864
0.26952	0.99528	213.8821	10.24186
0.31444	0.95036	235.8304	13.17501
0.35936	0.90544	253.8647	16.2086
0.40428	0.86052	267.9852	19.24893
0.4492	0.8156	278.1917	22.20227
0.49412	0.77068	284.4842	24.97492
0.53904	0.72576	286.8628	27.47317
0.58396	0.68084	285.3275	29.60331
0.62888	0.63592	279.8782	31.27162
0.6738	0.591	270.5149	32.3844
0.71872	0.54608	257.2377	32.84792
0.76364	0.50116	240.0465	32.56848
0.80856	0.45624	218.9412	31.45236
0.85348	0.41132	193.922	29.40586
0.8984	0.3664	164.9888	26.33526
0.94332	0.32148	132.1417	22.14687
0.98824	0.27656	95.38093	16.74702
1.03316	0.23164	42.45897	10.04207
1.07808	0.18672	3.986295	1.938486
1.123	0.1418	-11.3413	-7.65713
1.16792	0.09688	-21.9333	-18.8379
1.21284	0.05196	-30.3857	-31.6964
1.25776	0.00704	-37.4706	-46.3246
1.30268	-0.03788	-43.785	-62.8127
1.3476	-0.0828	-49.5471	-81.2486
1.39252	-0.12772	-54.6439	-101.716
1.43744	-0.17264	-59.4799	-124.292
1.48236	-0.21756	-63.8394	-149.043
1.52728	-0.26248	-67.9264	-176.013
1.5722	-0.3074	-71.777	-205.219
1.61712	-0.35232	-75.2482	-236.625
1.66204	-0.39724	-78.4912	-270.113

x(m)	ξ (m)	$\int_{L_K} R(\xi) f_{HD}^{2D} \xi d\xi$	$\int_{L_K} R(\xi) f_B^{2D} \xi d\xi$
1.70696	-0.44216	-81.3138	-305.433
1.75188	-0.48708	-83.7293	-342.126
1.7968	-0.532	-85.7825	-379.403
1.84172	-0.57692	-87.0684	-415.974
1.88664	-0.62184	-87.4731	-449.803
1.93156	-0.66676	-86.477	-477.786
1.97648	-0.71168	-83.5914	-495.41
2.0214	-0.7566	-78.2191	-496.486
2.06632	-0.80152	-69.8245	-473.243
2.11124	-0.84644	-57.7197	-417.153
2.15616	-0.89136	-41.6833	-320.824
2.20108	-0.93628	-22.0829	-180.785
2.246	-0.9812	0	0

The centers of hydrodynamic and hydrostatic pressure are computed using Equations (15) and (18). For the current condition (L_K=2.246), it is shown that LC_{HD}=0.1944 m and LC_B=-0.49 m. Subsequently, it is checked whether or not the pitch equation is satisfied. The computed values are displayed in Table A. 7. An error associated with the pitch moment is calculated again. When this error is negative the trim angle should decrease; otherwise it should increase.

Table A. 7. Checking the pitch equation error.

LC_{HD} (m)	-0.49
LC_B (m)	0.1944
M_B(N-m)	-260.697
M_{HD}(N-m)	159.6667
$\varepsilon = M_{HD} - M_B$(N-m)	-101.03

APPENDIX A.1: THE COMPUTED TRIM ANGLE AND ITS CORRELATION WITH EXPERIMENTAL DATA

For the initial trim angle of 4.1, the error associated with the pitch moment is equal to -101.03. Therefore, a new trim angle is guessed and the keel wetted length related to this trim angle is computed again (by producing similar tables to Table A. 2. through A. 5). Then, the error of satisfying the pitch equation by each guess is checked. As the sign of the error changes, the correct trim angle is to be between the last two guesses. At this stage, the trim angle is re-guessed by the 0.2 step size and the correct trim angle is found to be between 3.5 and 3.3, since the error changes sign when the trim is changed from 3.5 to 3.3 (Table A. 8). Using mathematical computations, the correct trim angle is estimated to be 3.352 and the keel wetted length is approximated to be 2.583. It should be noted that the trim angle measured by Metcalf et al. (2005) for this condition has been reported to be equal to about 3.13 degrees. Accordingly, the resultant error of 7.7% testifies to good accuracy of the proposed method.

Table A. 8. Errors for different trim angles.

No. Iteration	1	2	3	4	5
τ (deg)	4.1	3.9	3.7	3.5	3.3
L_K(m)	2.246186	2.42528	2.411342	2.535468	2.610539
ε (N-m)	-101.03	-49.784	-49.046	-13.1948	4.684451

CONTACT WITH THE AUTHOR

Parviz Ghadimi

e-mail: pghadimi@aut.ac.ir

Amirkabir University of Technology
424 Hafez Ave.
3314 Tehran

ISLAMIC REPUBLIC OF IRAN